Impact of CO_2-Induced Warming on Hurricane Intensities as Simulated in a Hurricane Model with Ocean Coupling

THOMAS R. KNUTSON AND ROBERT E. TULEYA

NOAA Geophysical Fluid Dynamics Laboratory, Princeton, New Jersey

WEIXING SHEN AND ISAAC GINIS

Graduate School of Oceanography, University of Rhode Island, Narragansett, Rhode Island

(Manuscript received 27 April 2000, in final form 30 October 2000)

ABSTRACT

This study explores how a carbon dioxide (CO_2) warming–induced enhancement of hurricane intensity could be altered by the inclusion of hurricane–ocean coupling. Simulations are performed using a coupled version of the Geophysical Fluid Dynamics Laboratory hurricane prediction system in an idealized setting with highly simplified background flow fields. The large-scale atmospheric boundary conditions for these high-resolution experiments (atmospheric temperature and moisture profiles and SSTs) are derived from control and high-CO_2 climatologies obtained from a low-resolution (R30) global coupled ocean–atmosphere climate model. The high-CO_2 conditions are obtained from years 71–120 of a transient $+1\%\ yr^{-1}$ CO_2-increase experiment with the global model. The CO_2-induced SST changes from the global climate model range from $+2.2°$ to $+2.7°C$ in the six tropical storm basins studied. In the storm simulations, ocean coupling significantly reduces the intensity of simulated tropical cyclones, in accord with previous studies. However, the net impact of ocean coupling on the simulated CO_2 warming–induced intensification of tropical cyclones is relatively minor. For both coupled and uncoupled simulations, the percentage increase in maximum surface wind speeds averages about 5%–6% over the six basins and varies from about 3% to 10% across the different basins. Both coupled and uncoupled simulations also show strong increases of near-storm precipitation under high-CO_2 climate conditions, relative to control (present day) conditions.

1. Introduction

The possibility of more intense tropical cyclones in a greenhouse gas–warmed climate has been suggested by both theoretical studies of the maximum potential intensity (MPI) of tropical cyclones (Emanuel 1987; Holland 1997; Henderson-Sellers et al. 1998) and by simulation studies with hurricane models (Knutson et al. 1998; Knutson and Tuleya 1999; Walsh and Ryan 2000). For example, Henderson-Sellers et al. (1998) conclude that for a doubled-CO_2 climate ''the MPI of cyclones will remain the same or undergo a modest increase of up to 10%–20%.'' Knutson and Tuleya (1999) simulated a 5%–11% increase of intensity under high-CO_2 conditions for a sample of model-generated typhoon case studies in the NW Pacific basin. For these types of studies, the large-scale environmental boundary conditions for the high-CO_2 climates are based on simulations by low-resolution global climate models.

One limitation of the high-resolution simulation studies to date has been the neglect of the effect of the tropical cyclone on the underlying ocean. It is now well-established that hurricane–ocean coupling can have an important impact on the intensity of the storms, primarily through the mixing of cooler subsurface ocean waters to the surface in the vicinity of the storm (Bender et al. 1993; Schade and Emanuel 1999; Emanuel 1999; Bender and Ginis 2000). This ''cool wake'' induced by the storm can then reduce the intensity of the storm, with the degree of reduction of intensity dependent on the magnitude of the cool wake. The cool wake magnitude in turn depends on such factors as the mixed layer depth and degree of stratification in the ocean, and the storm's size, intensity, and translation speed (Ginis 1995). An example of a cool wake induced by a simulated hurricane in one of our coupled experiments is illustrated in Fig. 1. The cooling induced in the SST field by the hurricane is clearly evident, with a local magnitude of up to 4°C or more in the wake of the moving storm. Comparisons between observed cool wakes and those simulated by a coupled version of the Geophysical Fluid Dynamics Laboratory (GFDL) hurricane model (e.g., Bender and Ginis 2000, Figs. 4 and

Corresponding author address: Thomas R. Knutson, NOAA Geophysical Fluid Dynamics Laboratory, P.O. Box 308, Forrestal Campus, U.S. Rt. 1, Princeton, NJ 08542.
E-mail: tk@gfdl.gov

© 2001 American Meteorological Society

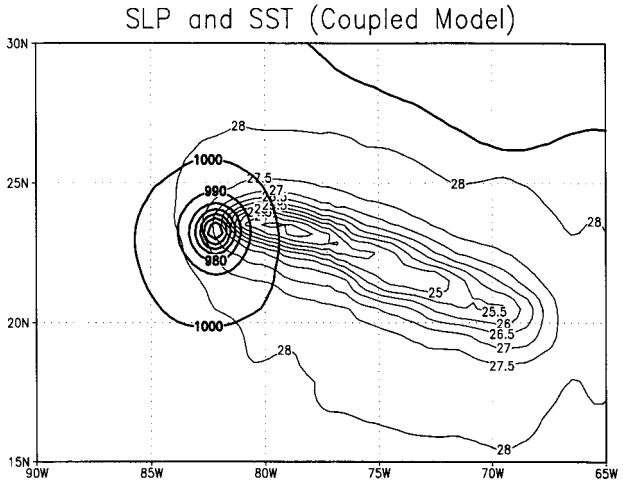

FIG. 1. SSTs (light contours; °C) and sea level pressure (dark contours; mb) at hour 72 for one of the idealized coupled hurricane model/ocean model cases (using the NW Atlantic highly stratified ocean temperature vertical profile). The ''cool wake'' in SSTs induced by the hurricane is indicated by the lower SSTs to the east-southeast of the storm. The storm motion is toward the west-northwest.

14) suggest that the model simulates fairly realistic hurricane-generated cool wakes in terms of magnitude and spatial extent [see also the recent example in Wentz et al. (2000)].

In a recent study, Shen et al. (2000) explored the sensitivity of simulated tropical cyclone intensities over a large parameter space, varying both atmospheric lapse rates and sea surface temperatures (SSTs) in combination. Their simulations indicated that increasing either SST or convective available potential energy (CAPE) tended to produce stronger storms, while enhanced upper-tropospheric warming (relative to the surface warming) tended to produce weaker storms. They also performed experiments with ocean coupling that indicated that the inclusion of ocean coupling led to reductions of storm intensity with a greater reduction occurring for stronger storms. They proposed that this mechanism may moderate the CO_2 warming–induced increases in storm intensity seen in experiments without ocean coupling (e.g., Knutson and Tuleya 1999). However, because their study examined the simultaneous variation of several parameters, the results were difficult to interpret quantitatively in terms of CO_2-induced boundary conditions as projected from particular global climate models. In this study, the importance of this negative ocean coupling feedback is assessed quantitatively for the specific case of the CO_2-induced changes in large-scale boundary conditions projected by the GFDL R30 global climate model. This model is the same one used for the simulations without ocean coupling by Knutson et al. (1998) and Knutson and Tuleya (1999). The results will show that while ocean coupling has an important impact on the intensity of tropical cyclones, its simulated impact on the CO_2-induced intensification of tropical cyclones is quite minor for the GCM boundary conditions examined here.

2. Methodology

Our idealized tropical cyclone modeling approach follows that used in Shen et al. (2000) and Knutson and Tuleya (1999). A regional hurricane prediction model is coupled to a regional ocean model for a series of 72-h coupled experiments. The large-scale environmental conditions are derived from a lower-resolution global climate model. By using idealized environmental flow fields, this approach does not consider the influence of storm interaction with transient flow features, as was examined in Knutson and Tuleya (1999). Each of the models involved in the study is described briefly below.

a. Hurricane model

For the idealized experiments, the GFDL Hurricane Prediction System (Kurihara et al. 1998) is used. This system, currently used operationally for hurricane prediction at the U.S. National Centers for Environmental Prediction (NCEP), consists of an 18-level, triply nested-moveable-mesh atmospheric model with a model-generated initial vortex. The outer grid covers a 75° × 75° region at a resolution of 1°, while the innermost grid covers a 5° × 5° region at a resolution of 1/6°, or about 18 km. The regional hurricane model simulates significantly stronger, more compact hurricanes, and a more realistic representation of hurricane intensities and structure than does the global climate model from which the large-scale boundary conditions are derived.

For each experiment, an initial disturbance is embedded in an idealized zonal flow with no other initial disturbances, no land, and uniform initial SST. The large-scale thermodynamic atmospheric environments for the experiments are derived from the time-averaged, area-averaged SST, temperature, and water vapor from the climate model as described below. For most experiments the idealized flow environment used consists of a 5 m s^{-1} easterly flow at all levels, although other flow environments are also tested, as described later in the report. The surface pressure and the temperature fields are computed at the end of the vortex insertion procedure by solving a form of the reverse balance equation, using the climate model–derived temperatures as a reference boundary condition at the central latitude of the east–west channel. The temperature profiles at other latitudes along the boundaries could vary from the reference profile, for example, because of the presence of vertical wind shear in some experiments.

The initial vortex for the experiments is an idealized hurricane initial condition based on Hurricane Fran (2 September 1996) with maximum surface wind speeds of approximately 35 m s^{-1} at a radius of 55 km. The same initial disturbance is used for each experiment except for small random perturbations to the maximum

intensity of the vortex. These runs with small perturbations to the initial conditions are used to create an ensemble of results in order to test the robustness of the simulations to small variations in initial conditions. The sample of randomly perturbed initial maximum intensities is derived from a Gaussian distribution with mean of 35 m s^{-1} and standard deviation of 0.5 m s^{-1}. For each experiment, the resulting disturbance vortex, including a beta-effect related asymmetric component, is superimposed on the environmental flow to create the total initial wind distribution. The average initial intensity, in terms of central pressure, is 968 mb with a range of initial intensities of approximately 965–971 mb. Other details of the initial condition are as follows: the gale-force surface winds extend out about 110 km from the storm center in the NE quadrant, where the winds are about 10 m s^{-1} stronger than in the SW quadrant for the 5 m s^{-1} environmental flow cases. The vertical structure of the initial disturbance is fairly deep, with maximum winds at about 950 mb and the main falloff with pressure occurring between 400 and 200 mb. The maximum radial shear (surface winds) approaches 1 m s^{-1} km^{-1} in the 1/6° inner nest. The relative vorticity maximum is 0.0017 s^{-1}.

b. Regional ocean model

For the coupled hurricane model experiments the atmospheric model described above is coupled to a 1/5°-resolution 23-level regional version of the Princeton Ocean Model (Bender and Ginis 2000). Separate experiments were run for atmosphere and ocean environmental conditions from each of six tropical storm basins for both control and high-CO_2 conditions.

Because of the coarse vertical resolution of the oceanic component of the global climate model, the detailed near-surface temperature stratification (vertical temperature gradient) is not sufficiently well-simulated in the climate model for the purposes of the present study. Therefore, to improve the realism of the ocean response to the storms, the ocean thermal stratifications for the control cases are based on observed (U.S. Navy Generalized Digital Environmental Model; GDEM) seasonal-mean climatologies. The absolute temperature values at each vertical level are adjusted from the GDEM values so that the adjusted SST value matches that from the climate model control run for each basin without altering the vertical temperature gradients. The ocean temperature profiles for the high-CO_2 cases are constructed by adding the high-CO_2-minus-control differences from the climate model to the control profiles derived from the GDEM climatology as described above.

Both a basin-average stratification and a strong temperature stratification sets of experiments are run for each basin, with the strong stratification profiles selected based on a visual inspection of maps of near-surface temperature stratification from the GDEM climatologies. As examples, the strong stratification profile for the NW Atlantic basin is obtained from the central Gulf of Mexico (July–September season) and the strong stratification profile for the NW Pacific basin is obtained from the South China Sea (July–September season). The ''strong stratification'' profiles differ from the basin mean profiles in more than cooler temperatures at depth; they also exhibit much shallower mixed layers. The strong stratification profiles selected, being based on seasonal-mean climatologies, do not represent absolute upper limits on possible temperature stratification in the basins. For example, stronger stratifications could occur in association with transient oceanic variability not examined here. The vertical profiles used in the study for control simulations in each basin (adjusted to match the climate model SSTs) are shown in Fig. 2 (Control Profiles).

For the high-CO_2 cases, a slight increase in upper-ocean vertical temperature gradient or stratification is

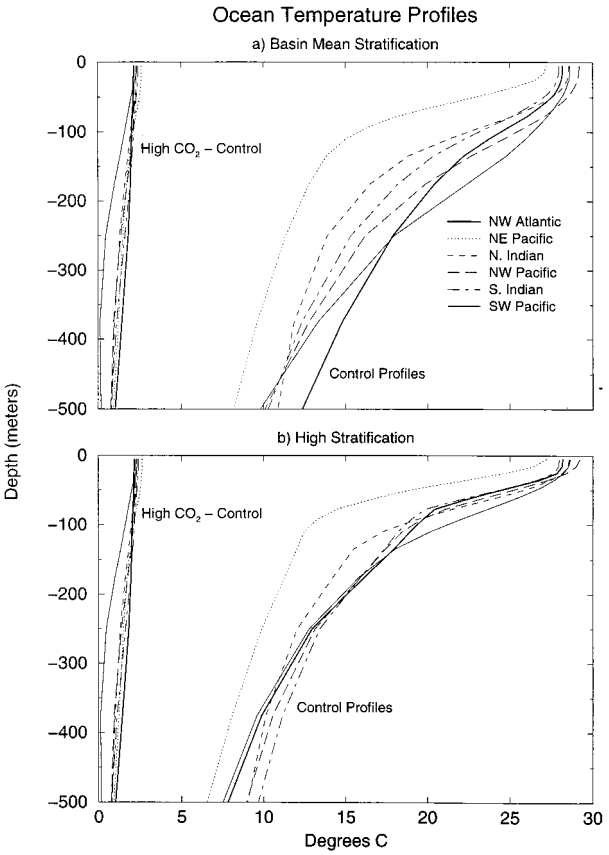

FIG. 2. Vertical profiles of ocean temperature used as initial conditions in the coupled simulations based on (a) tropical storm basin mean averages; or (b) highly stratified climatological profiles obtained from each basin using the GDEM climatologies (see text). The profiles have been adjusted by a constant amount at each level so that they match the SST value for that basin as simulated in the global climate model control run. The six individual basins are identified by the various line types (see legend). The difference profiles for each basin (High-CO_2 − Control) are shown by the curves on the left side of each panel.

incorporated, based on the global climate model simulations of the vertical structure of CO_2-induced ocean temperature changes in these basins (Fig. 2, High-CO_2 − Control curves). The climate model's CO_2-induced ocean temperature profile changes are fairly similar between different basins. Because of the coarse horizontal and vertical resolution of the global climate model, the basin-mean CO_2-induced changes from the model are applied to both the basin-averaged and high-stratification observed profiles. The CO_2-induced enhancement of the vertical temperature gradient should enhance the effect of ocean coupling on storm intensities for the high-CO_2 cases, although a caveat is that the upper ocean is only crudely resolved in the global coupled climate model used to define the profile changes for this study. If the upper-ocean stratification were much increased under high-CO_2 conditions in real-world climate change, this could offset some or all of the effect of higher SSTs on storm intensity. Therefore, it will be important to revisit the present problem in the future as climate change simulations with models capable of more realistic representations of the upper-ocean thermal stratification and mixed layer become available.

The ocean profiles thus obtained provide the initial ocean states used for the coupled hurricane model experiments. At the initial time, the ocean is specified to be motionless with horizontally uniform temperatures based on the above profiles. For the uncoupled experiments described in the report, the SSTs are held fixed at their initial values (based on either control or high-CO_2 conditions) during the entire 72-h experiment.

c. Global climate model

The large-scale boundary conditions (e.g., SST, atmospheric temperature, and water vapor, and changes to the ocean temperature profiles) for the hurricane model experiments are derived from climatologies of a low-resolution coupled ocean–atmosphere global climate model. The global model used is the GFDL R30 coupled ocean–atmosphere climate model (Manabe et al. 1991; Knutson and Manabe 1998). The R30 spectral atmospheric component's transform grid has resolution of about 2.25° latitude (250 km) × 3.75° longitude (400 km) and 14 finite difference levels in the vertical. The oceanic component of the global climate model is an 18-level finite difference global ocean general circulation model (GCM) (Modular Ocean Model, version 1) with the same latitudinal resolution and 2 times the longitudinal resolution of the atmospheric model's transform grid. The top layer of the ocean model has a thickness of 32 m. The model uses a flux adjustment technique for heat and salinity fluxes at the ocean surface to reduce model drift so that the CO_2 perturbations and internally generated variability occur relative to a reasonably realistic control run seasonal cycle (Manabe et al. 1991).

In addition to spatial resolution, the global model differs from the regional hurricane model in terms of model physics, diurnal variation, and so on. These model differences can be expected to lead to differences between the regional and global model climatologies. Thus the environmental fields in the regional model will tend to adjust toward the regional model's climatology during the 3-day integrations. In our study, since these adjustments occur in both the control and high-CO_2 cases, it is assumed that their net effect on the sensitivity results (high-CO_2 minus control) is small in comparison with the CO_2-induced changes in intensity. We also note that the climate sensitivity of a hypothetical global version of the hurricane model could be different from that of the R30 global climate model, but this effect is not investigated here.

Two 120-yr experiments were previously carried out with the global model (Knutson and Manabe 1998): a control integration with CO_2 constant at present-day levels, and a transient CO_2-increase experiment in which atmospheric CO_2 levels increased at $+1\%\ yr^{-1}$ compounded (that is, by a factor of 2.57 by year 95). A $+1\%\ yr^{-1}$ compounded increase of CO_2 represents an idealized greenhouse gas forcing scenario, rather than a forecast of future concentrations. As noted by Schimel et al. (1996), other anthropogenic radiative forcings besides greenhouse gases may have important effects on global climate although their quantification remains uncertain.

Data from the years 71–120 of these two experiments are averaged over the appropriate tropical cyclone season for each basin to provide the large-scale control and high-CO_2 environmental conditions for the idealized experiments. The specific region definitions used are as follows: (i) NW Pacific: July–November; 8°–26°N, 124°–161°E; (ii) NW Atlantic: July–November; 10°–26°N, 49°–79°W; (iii) NE Pacific: July–November; 10°–19°N, 101°–131°W; (iv) North Indian: May–June, September–December; 8°–19°N, 64°–94°E; (v) SW Pacific: December–March; 8°–19°S, 150°E–150°W; (vi) South Indian: December–March; 8°–19°S, 60°–120°E.

The CO_2-induced SST changes for the different tropical storm basins vary from 2.2° (NW Atlantic and NW Pacific) to 2.7°C (NE Pacific). Further details on the tropical simulations from these experiments are presented in Knutson and Manabe (1998) and Knutson and Tuleya (1999).

3. Simulation results

a. Storm intensity changes

In this section the simulated storm intensities are compared for various basins, ocean thermal stratifications, climate boundary conditions (control and high CO_2), and so forth. For the intensity comparisons, the central surface pressure averaged over the final 24 h of each experiment (i.e., hours 49–72) is used. Similar results (not shown) are obtained using the maximum surface

wind speed as the intensity measure. Although the temporal evolution of the intensities is not shown here, most of the intensification occurs in the first 24 h of the simulations, as in the examples shown by Shen et al. (2000, their Fig. 3).

Figure 3 presents a summary of the tropical cyclone intensity results (central surface pressures) for the main set of experiments performed for the study. Each diagram in Fig. 3 shows the results for one of the six basins studied. On each diagram (basin) are three sets of results: 1) without ocean coupling, 2) with ocean coupling using the basin-mean ocean temperature vertical stratification, and 3) with ocean coupling using a strong ocean temperature stratification (see Fig. 2 and the horizontal axis labeling on Fig. 3). The circles linked by a vertical line segment show the ensemble means of the surface pressure results for a given ocean stratification for either high-CO_2 (dark circles) or control (light circles) conditions. Each ''+'' symbol depicts the central surface pressure, averaged over hours 49–72, for a single model integration. The + symbols to the left and right of each connected set of circles represent the individual elements (integrations) of the ensemble for the control and high-CO_2 samples, respectively. The individual elements of the ensembles differ only by small changes in the specified initial vortex intensity.

Several notable results of the experiments are clearly shown in Fig. 3, of which we note four here. First, the storms are generally weaker for the ocean coupling cases than for the uncoupled cases. For example, the control run storms (open circles) for the coupled cases (average or strong stratification) have higher central surface pressures than the control run storms without ocean coupling. Second, stronger vertical gradients of ocean temperature lead to greater coupling-induced reductions in hurricane intensity, as seen by comparing the average and strong stratification cases. The effect of increased stratification on the turbulent mixing rate is rather minor for hurricane conditions, whereas the increased temperature stratification leads to marked increases of heat flux into the mixed layer due to the larger temperature gradients in the thermocline below. Third, for each individual type of ocean coupling condition (no coupling, average ocean stratification, or strong ocean stratification) the high-CO_2 storms (dark circles) tend to be more intense than the control storms (light circles). Thus, a CO_2 warming–induced intensification of hurricanes still occurs even when the hurricane–ocean coupling effects are included. Fourth, the CO_2-induced increase of intensity varies from basin to basin and is largest in the NE Pacific. The largest SST increase (2.7°C) occurs for the NE Pacific basin, and as noted in Knutson and Tuleya (1999, see their Fig. 3), a slightly larger enhancement of the lower tropospheric equivalent potential temperature occurs in the NE Pacific than in the other basins.

The main purpose of the present study is to determine whether ocean coupling alters the CO_2-induced intensification of hurricanes as simulated in previous studies that did not include ocean coupling. If such an effect were present, the separation between the control and high-CO_2 ensemble mean intensities (solid and open circles connected by a line segment in Fig. 3) would be different in the coupled and uncoupled cases. Inspection of Fig. 3 suggests that a slight reduction of the CO_2-induced intensification may occur in the ocean coupling cases for three of the six basins (NW Pacific, NE Pacific, and SW Pacific) but the effect is relatively small and nonsystematic; such an effect is not even present for the NW Atlantic, North Indian, and South Indian cases. The relatively minor change for the SW Pacific basin is notable in that the ocean thermal stratification is enhanced more in the global climate model high-CO_2 simulation in that basin than in any of the other basins (Fig. 2).

The intensity results for the basins are combined to form a six-basin average set of results. The six-basin mean intensity change (high-CO_2 minus control) is -8.3 mb (uncoupled) versus -8.4 mb (average stratification) and -8.3 mb (strong stratification). In terms of maximum surface wind speed (again averaged over hours 49–72 for each case) the six-basin mean intensity change (high-CO_2 minus control) is 2.6 m s^{-1} or 5.3% (uncoupled) versus 2.8 m s^{-1} or 5.9% (average stratification) and 2.8 m s^{-1} or 6.1% (strong stratification). The six-basin mean results suggest that the effect of ocean coupling on the CO_2-induced intensification is essentially negligible, at least for the case of storm movement at $\sim$5 m s^{-1}. The range of CO_2-induced intensifications seen across the various basins is about 3%–10% in terms of maximum surface wind speeds and 4–14 mb in terms of central surface pressure, with similar ranges for coupled and uncoupled simulations.

The statistical significance of the ocean coupling effects on the CO_2-induced intensification was assessed (appendix) and found to be fairly marginal and basin-dependent but with a tendency to indicate a slight reduction of the CO_2-induced intensification in some basins. (In contrast, the CO_2-induced intensification was highly significant for each basin and for each ocean coupling type.) From these results we conclude that while ocean coupling appears to reduce the CO_2-induced intensification, this effect is relatively minor in percentage terms, at least for an environmental flow of 5 m s^{-1}.

To place the simulated CO_2-induced intensification in context, we have attempted to compare it with the interannual variability of tropical cyclone intensities in the real climate system. Since the idealized storm simulations do not include dynamical effects such as vertical shear, which can potentially inhibit development, they can be regarded as potential intensities for the time-averaged thermodynamic environment in each basin. As shown in Knutson and Tuleya (1999, Fig. 7 vs Fig. 11), they do not represent the upper-limit intensities for a basin, since transient weather and ocean fluctuations can lead to environments with larger potential intensities.

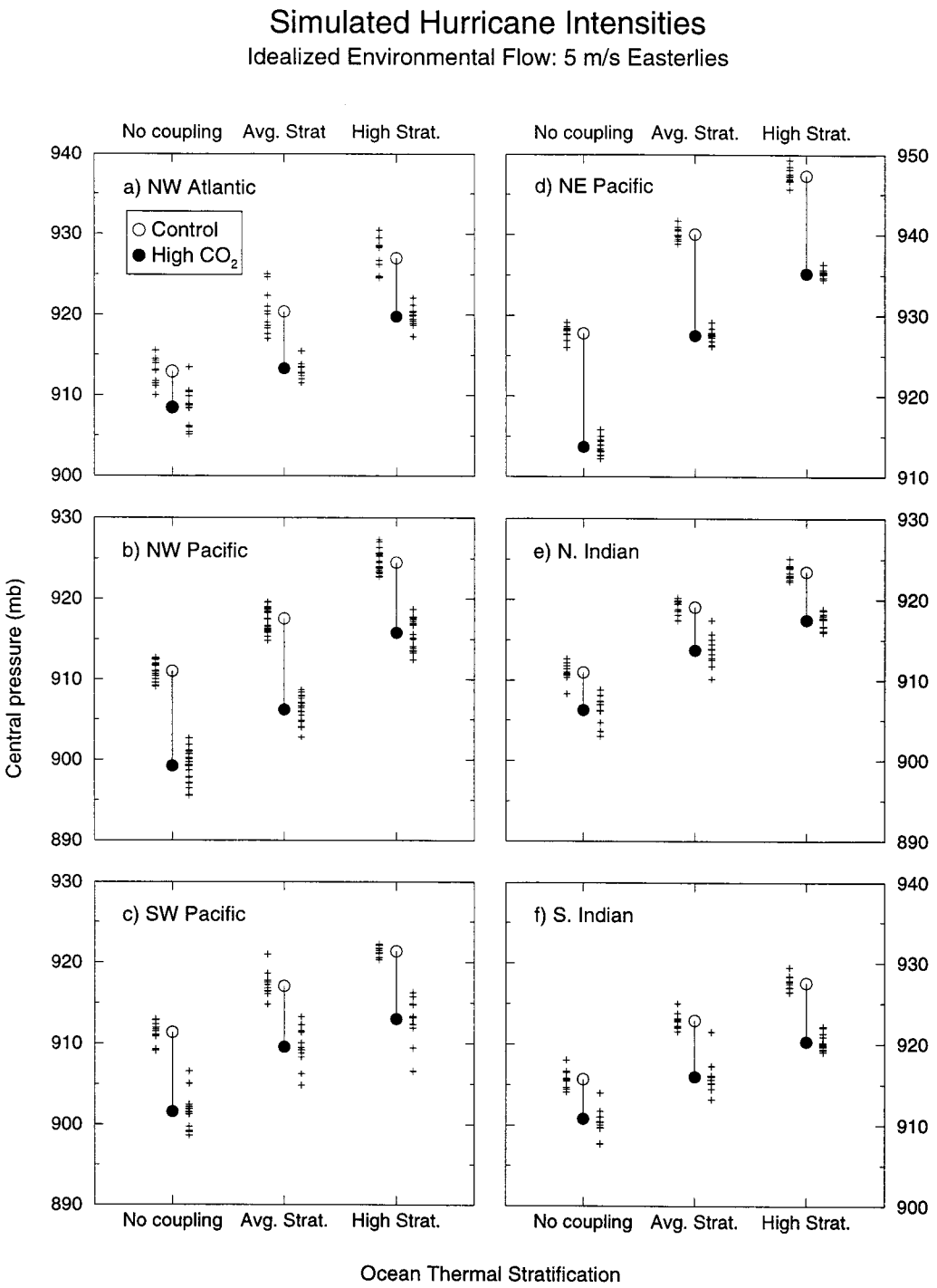

FIG. 3. Minimum central surface pressure (mb) comparisons of different idealized experiments run using average thermodynamic conditions (SST, atmospheric temperature, and moisture, vertical profile of ocean temperature) for the various tropical storm basins (a–f) as described in the text. A 5 m s^{-1} easterly environmental atmospheric flow and the same initial storm vortex—aside from a small random perturbation—is used for each experiment shown. The horizontal axis qualitatively identifies the ocean thermal stratification for each group of experiments (i.e., no coupling, average temperature stratification, or strong temperature stratification). The ensemble mean central surface pressures for the high-CO_2 and control experiments are depicted by the dark-filled and unfilled circles, respectively. Each + symbol represents a single integration or element of the ensemble. The + symbols to the left and right of the ensemble mean results correspond to the control and high-CO_2 experiments, respectively. Note that although the absolute central pressure scale (vertical axis labeling) varies between the different diagrams, the relative scaling (pressure difference between tic marks) is the same for all diagrams. The central surface pressures are averages over the final 24 h of each experiment (i.e., hours 49–72).

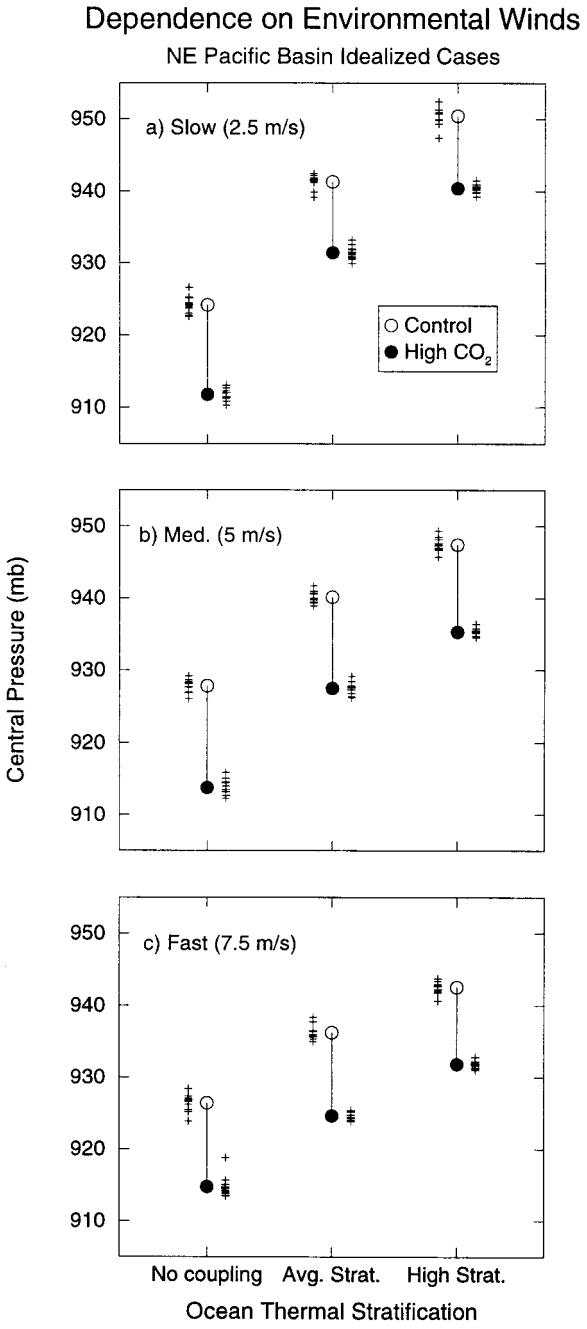

FIG. 4. As in Fig. 3 but for the NE Pacific only, using an easterly atmospheric environmental flow field of (a) 2.5, (b) 5.0, or (c) 7.5 m s^{-1}, respectively.

However, as a rough comparison of our simulation results to real-world variability, we can compare the relative (percentage) CO_2-induced changes in simulated storm intensities with the relative interannual variability (i.e., the interannual standard deviation divided by the long-term mean) of the annual strongest storm in the observed record for a given basin. Using the observed tropical cyclone data of C. J. Neumann (available from NCAR, http://dss.ucar.edu/datasets/ds824.1), we estimate a relative variation of 7.1% (5.4 m s^{-1} standard deviation and 75.6 m s^{-1} mean) for surface wind speeds of the annual strongest storm in the NW Pacific basin (1953–92), and a relative variation of 15.5% (10.1 m s^{-1} standard deviation and 65.1 m s^{-1} mean) in the NW Atlantic basin (1943–92). In comparison, for our idealized simulations, the relative CO_2-induced change in the NW Pacific is 6.7% for the basin mean ocean thermal stratification, or comparable to the observed relative interannual variability. In the NW Atlantic, the simulated relative CO_2-induced change (4.7%) is less than one-third of the observed interannual variability estimate. These results suggest that a CO_2-induced storm intensification such as that simulated here would be difficult to detect in the real world even after many decades of future climate change, particularly in basins with higher interannual variability such as the NW Atlantic. In fact, Landsea et al. (1996) have noted an apparent *downward* trend in the frequency of intense Atlantic hurricanes during the past half century. SSTs in the NW Atlantic basin have exhibited a slight cooling trend during the past half century (e.g., Knutson et al. 1999).

Storm translation speeds are quite variable from case to case in the real world (Elsberry 1995) although 5 m s^{-1} is a reasonable ''typical'' value. As shown by Bender et al. (1993) a hurricane's translation speed has an important impact on storm intensity in coupled hurricane–ocean experiments since the mixing-induced cooling occurs closer to the storm center for more slowly propagating storms. Therefore, as a sensitivity case, ensemble experiments are performed for the NE Pacific basin for alternative environmental flows of 2.5 m s^{-1} (slower storm propagation) and 7.5 m s^{-1} (faster propagation). The results of these additional experiments are summarized in Fig. 4.

As expected, the effect of ocean coupling on storm intensity is enhanced in the case of the weaker environmental flow (2.5 m s^{-1} easterlies). For this slow propagation case, the control storms have weakened about 25 mb (from about 925 mb with no coupling to about 950 mb for the high ocean stratification condition). This weakening is greater than the ~15-mb weakening simulated for the faster-moving control storms (embedded in 7.5 m s^{-1} easterlies). There also appears to be some reduction of the CO_2-induced storm intensification effect, from about 12 mb in the uncoupled case to about 10 mb in the average or strong stratification cases. However, this effect remains relatively minor and is negligible in terms of the percentage change in maximum surface wind speeds.

Storm size is another factor that has important impacts on the ocean feedback process. For example, a larger storm produces upper-ocean mixing over a larger area—and for a longer time duration in a given region—than a smaller storm propagating at the same speed. Although this effect is not explicitly analyzed here, the slow storm propagation speed (2.5 m s^{-1} environmental flow) sen-

sitivity test provides an indication of this potential effect of storm size. Even for the case of a very slowly moving storm, ocean coupling has only a relatively minor effect on the CO_2-induced storm intensification signal. Other effects of storm size, such as its effect on storm propagation or on ocean coupling via ocean surface wave responses, are not analyzed in this study. However, there is at present no evidence to indicate substantial changes in storm sizes in a high-CO_2 climate.

b. Precipitation changes

In addition to storm intensity, other aspects of hurricanes could be altered in a CO_2-warmed climate. We have also examined the simulated near-storm precipitation in our idealized model runs. Two different measures of storm precipitation are examined: 1) a measure of the maximum local precipitation rate in the storm and 2) the precipitation rate of the mature storm averaged over the region within 100 km of the storm center. For measure 1, data are available from the model at 1-h intervals, so the local maximum precipitation rates at each hour are obtained and the resulting time series is averaged over hours 49–72 to create a single time-averaged maximum precipitation value for each integration. For measure 2, data are available only at 24-h intervals, so the area-averaged (100 km) precipitation rate is computed from the ''snapshot'' at the end of each integration (hour 72).

According to measure 1 (maximum precipitation rate), the precipitation in the high-CO_2 storms is enhanced by about 34% (with a range of 28%–45% across the six basins) relative to the control. Using measure 2 (area-averaged precipitation rate) the precipitation in the high-CO_2 storms is enhanced by about 17% (range of 9%–29%).

The effect of ocean coupling on these results appears to be relatively minor. For example, in the high-stratification ocean coupling cases, the precipitation is enhanced by 31% (range of 28%–34% across the six basins) according to measure 1 (maximum precipitation rate). Using measure 2 (area-averaged precipitation rate) the precipitation is enhanced by 19% (range of 9%–48%).

Precipitation from hurricanes can produce devastation in addition to that from the storm winds and storm surge at landfall, as in the recent example of Hurricane Mitch (1998) in Central America. Thus a CO_2-induced increase of storm precipitation such as that simulated in the present study could have important future societal consequences in addition to the simulated wind speed increases.

4. Analysis and interpretation of ocean coupling effects

In this section we briefly investigate the relationship between different ocean coupling-induced effects. In particular, we examine the magnitude of the cold SST wake generated by storms under various conditions in order to gain insight into why ocean coupling has only a minor effect on CO_2-induced intensification of hurricanes in our simulations.

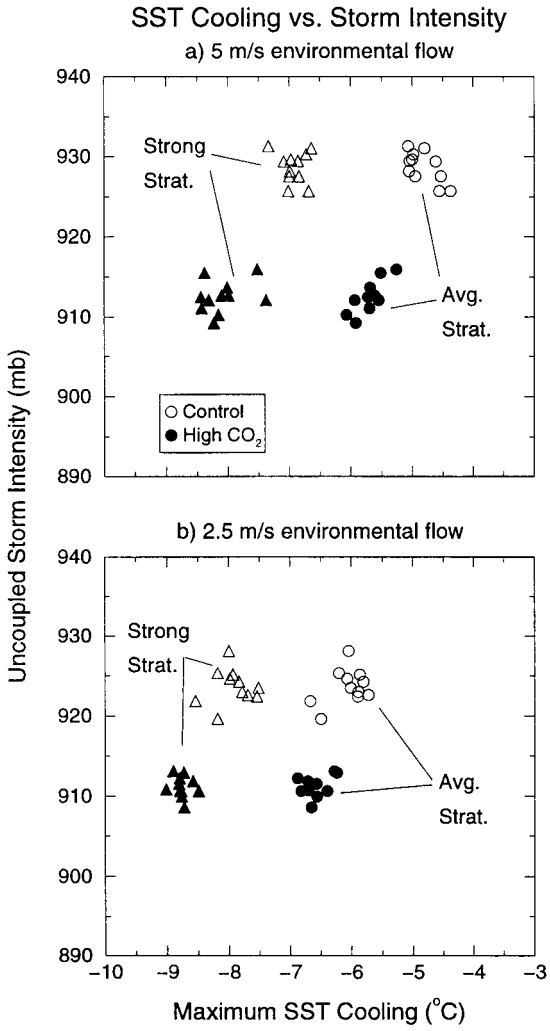

FIG. 5. Scatterplot of SST cooling (the maximum SST cooling at hour 72 anywhere within the 5° × 5° inner nest, °C) vs the uncoupled model hurricane intensity (mb) at hour 72 for various individual elements of the NE Pacific ensemble simulations using (a) 5 or (b) 2.5 m s^{-1} easterly atmospheric environmental flows. High-CO_2 and control cases are identified by solid-filled and unfilled symbols, respectively. Average and strong ocean temperature stratification conditions are identified by circles and triangles, respectively. Note that the hour-72 central pressures in this figure do not exactly match the results in Fig. 3 since the latter are based on averages over hours 49–72.

In Fig. 5 are scatterplots of hurricane intensity in the NE Pacific uncoupled experiments versus the magnitude of the cold wake simulated in the coupled experiments for the same initial conditions. Fig. 5a shows results for the default 5 m s^{-1} easterly environmental flow condition, and Fig. 5b shows results for 2.5 m s^{-1} easterly

flow, where the storm moves more slowly over the ocean surface. On each panel, results are shown for both average and strong ocean temperature stratification, denoted by circles and triangles, respectively. Dark-filled symbols refer to experiments run under high-CO_2 conditions, whereas unfilled symbols refer to experiments run under control climate conditions. The magnitude of the cold wake is represented by the maximum SST cooling at hour 72 found anywhere in the $5° \times 5°$ inner nest surrounding the storm. Similar results are obtained using other cold-wake measures such as the SST cooling within 100 km of the storm center or the average cooling over the entire inner nest.

The results in Fig. 5 indicate that for a given thermal stratification (i.e., strong or average stratification), a stronger storm produces a stronger cold wake upon incorporation of ocean coupling. For example, the SST coolings produced by the high-CO_2 storms (dark triangles) are systematically stronger than those produced by the control storms (unfilled triangles). (Although the ocean stratifications were slightly stronger for the high-CO_2 conditions than for the control, based on the climate model simulations, we believe that this effect is of secondary importance and can be neglected for the purposes of the present discussion.) The results in Fig. 5 also show that stronger ocean thermal stratification leads to stronger SST cooling (e.g., comparing average and strong stratification results for the control runs) and that more slowly propagating storms produce stronger cooling (comparing the cooling magnitudes in Fig. 5a with those in Fig. 5b).

Figure 6 shows scatterplots of the coupling-induced change in central surface pressure versus the cold-wake magnitude induced by ocean coupling. All cases for all basins are shown in Fig. 6a whereas the results for the NE Pacific 5 m s^{-1} easterly flow cases are shown in Fig. 6b. The results show that in general the stronger the magnitude of the cold wake, the stronger the coupling induced reduction in storm intensity. However, the relationship is not a perfect one, but is characterized by a considerable degree of scatter about a generally linear relationship. Close inspection of Fig. 6b suggests the reason why ocean coupling does not produce a large impact on the CO_2-induced intensification of hurricanes. The difference in storm intensity between control and high-CO_2 storms, while significant, still only produces about 1°C difference in the maximum SST cooling, as compared with an overall maximum SST cooling of 5°–7°C in the control cases. This relatively small change in the magnitude of the cold wake is not pronounced enough to produce a large difference in the coupling-induced storm intensity reduction. In other words, the stronger storms in the high-CO_2 conditions produce stronger cold wakes as expected, but the increase in the wake magnitude is sufficiently small that it has a relatively minor negative feedback onto the CO_2-induced intensification. In fact, the small negative feedback is difficult to detect in our experimental results, probably because of sampling fluctuations or ''noise.''

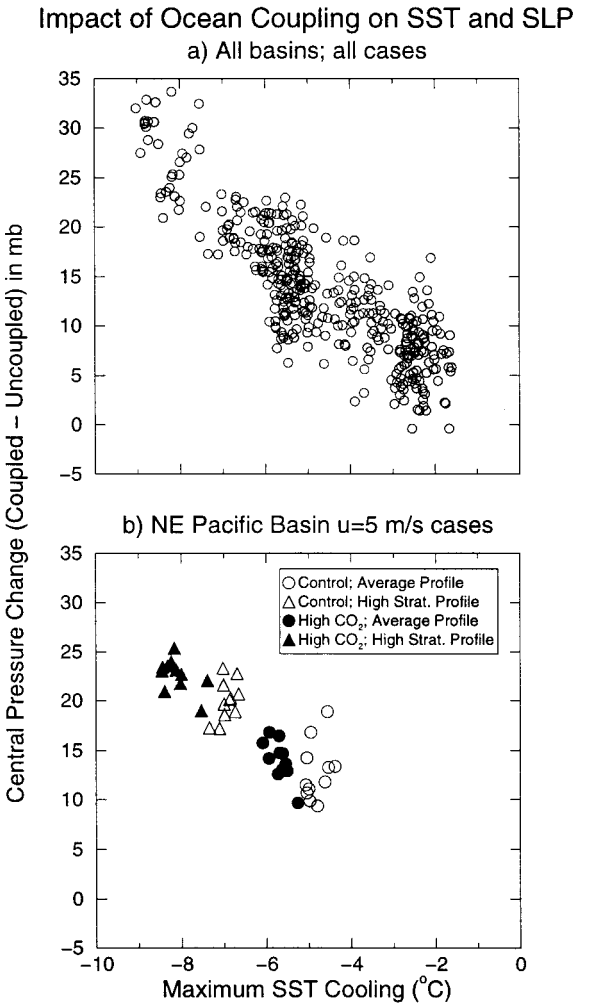

FIG. 6. Scatterplot of maximum SST cooling (in °C, see text) versus the ocean coupling-induced change in central surface pressure (i.e., coupled minus uncoupled central surface pressure) in mb for h 72. Results are shown for (a) all basins and all cases; or (b) NE Pacific ensemble simulations for 5 m s^{-1} easterly environmental atmospheric flow only. In (b) the high CO_2 and control cases are identified by solid-filled and unfilled symbols, respectively, while average and strong ocean temperature stratification conditions are identified by circles and triangles, respectively.

5. Discussion and conclusions

In this study, we use a coupled atmosphere–ocean version of the GFDL hurricane prediction system to explore the sensitivity of hurricane intensities to CO_2-induced warming. The changes in large-scale environmental conditions due to increasing CO_2 used in the experiments are obtained from a GFDL global climate model. We attempt to quantify how the inclusion of ocean coupling affects the CO_2 warming–induced enhancement of hurricane intensities simulated in previous studies without ocean coupling.

When ocean coupling is included, the simulated hurricanes produce a cold wake in the SST field as they propagate over the open ocean. Stronger storms produce stronger wakes, as do storms that propagate more slowly or storms that occur over ocean regions with stronger thermal stratification. The hypothesis examined in the present study is that the intensification of storms due to CO_2-induced warming would be partly mitigated by ocean coupling, since the stronger high-CO_2 storms should produce stronger cold wakes that should act as a negative feedback, limiting the intensity of the storms. In the experiments performed, the high-CO_2 storms do have slightly stronger cold wakes, but the effect is not strong enough to have more than a minor impact on the CO_2-induced intensification. Therefore, we conclude that the inclusion of ocean coupling, as simulated in our coupled modeling system, has only a minor impact on the simulated intensification of hurricanes in a CO_2-warmed environment.

In terms of hurricane-related precipitation, the idealized cases in the present study are characterized by pronounced CO_2-induced increases in near-storm precipitation, similar to those noted by Knutson and Tuleya (1999). The simulated increase is about 20% for precipitation averaged with 100 km of the storm center and about 30% for the maximum precipitation rate for the storm. Ocean coupling appears to have a relatively minor effect at most on these results.

Although additional physical processes are incorporated into our simulations examining the effect of CO_2-induced warming on hurricane intensities, other caveats still remain regarding our studies. For example, the large-scale boundary conditions (SSTs, lapse rates) used for the experiments are from a single global climate model forced by increasing greenhouse gases alone. Other climate models or other combinations of radiative forcings could produce different responses to what we simulate in our studies. The CO_2-induced changes in upper-ocean temperature vertical structures (e.g., mixed-layer depth changes) are only crudely resolved in the global climate model used in deriving the initial ocean conditions for the present study. Also, the present study does not address the question of possible changes in storm frequency or location of occurrence under high-CO_2 conditions.

Given these caveats, our simulation results incorporating ocean coupling continue to suggest that, with a CO_2-induced warming, hurricanes will have the potential to reach greater intensities. The simulated surface wind intensities in our experiments are enhanced by roughly +3% to +10% in response to a CO_2-induced tropical SST warming of 2.2°–2.7°C.

Acknowledgments. We thank Y. Kurihara, A. Rosati, K. Emanuel, and an anonymous reviewer for helpful comments on this manuscript. I. G. and W. S. were supported by the National Science Foundation through Grant ATM 9714412.

APPENDIX

Statistical Significance Tests

The statistical significance of the simulation results shown in Fig. 3 is analyzed using a nonparametric statistical test—the Kolmogorov-Smirnov distribution test (Siegel and Castellan 1988). For each basin and for each ocean coupling type, the high-CO_2 storms are significantly more intense ($p < 0.001$) than the control storms. However, here we examine the related question of whether ocean coupling leads to a statistically significant reduction in the CO_2-induced intensification. For this test, distributions are formed by computing the intensity difference between individual ensemble members from the control cases and individual ensemble members from the high-CO_2 cases for a given ocean coupling type. The distributions of these CO_2-induced intensity changes are then compared using the KS test (uncoupled versus average stratification and uncoupled versus strong stratification). The comparisons are done for both central surface pressure and maximum surface wind speeds using data averaged over hours 49–72 of each individual ensemble member. A one-sided test is used, based on the expectation from previous studies that ocean coupling should reduce the CO_2-induced intensification.

For central surface pressure, a significant effect ($p = 0.05$) of the expected sign is found for the NE Pacific and SW Pacific basins (average stratification) and NW Pacific and NE Pacific (strong stratification). For surface wind speed, only the NW Pacific strong stratification case is significant. Using a more stringent test ($p = 0.01$) only the NW Pacific strong stratification central pressure result is significant. Although ocean coupling is not expected to lead to any increase in the CO_2-induced intensification, the basins where a change of this sign occurred are tested, also using a one-sided test as a sensitivity test. Several ''significant'' changes are seen at the 0.05 level, although no ''significant'' changes are found at the 0.01 level. In summary, the statistical significance test results are marginal and basin-dependent, indicating that while the simulated effect of ocean coupling has a tendency overall to reduce the CO_2-induced intensification, the effect is relatively minor in percentage terms.

REFERENCES

Bender, M. A., and I. Ginis, 2000: Real-case simulations of hurricane–ocean interaction using a high-resolution coupled model: Effects on hurricane intensity. *Mon. Wea. Rev.*, **128,** 917–946.

——, ——, and Y. Kurihara, 1993: Numerical simulations of tropical cyclone–ocean interaction with a high-resolution coupled model. *J. Geophys. Res.,* **98,** 23 245–23 263.

Elsberry, R. L., 1995: Tropical cyclone motion. *Global Perspectives on Tropical Cyclones*, R. L. Elsberry, Ed., WMO Tech. Doc. No. TCP-38, 106–197.

Emanuel, K. A., 1987: The dependence of hurricane intensity on climate. *Nature*, **326,** 483–485.

——, 1999: Thermodynamic control of hurricane intensity. *Nature,* **401,** 665–669.

Ginis, I., 1995: Ocean response to tropical cyclones. *Global Perspectives on Tropical Cyclones,* R. L. Elsberry, Ed., WMO Tech. Doc. No. TCP-38, 198–260.

Henderson-Sellers, A., and Coauthors, 1998: Tropical cyclones and global climate change: A post-IPCC assessment. *Bull. Amer. Meteor. Soc.,* **79,** 19–38.

Holland, G. J., 1997: The maximum potential intensity of tropical cyclones. *J. Atmos. Sci.,* **54,** 2519–2541.

Knutson, T. R., and S. Manabe, 1998: Model assessment of decadal variability and trends in the tropical Pacific Ocean. *J. Climate,* **11,** 2273–2296.

——, and R. E. Tuleya, 1999: Increased hurricane intensities with CO_2-induced warming as simulated using the GFDL hurricane prediction system. *Climate Dyn.,* **15,** 503–519.

——, ——, and Y. Kurihara, 1998: Simulated increase of hurricane intensities in a CO_2-warmed climate. *Science,* **279,** 1018–1020.

——, T. L. Delworth, K. W. Dixon, and R. J. Stouffer, 1999: Model assessment of regional surface temperature trends (1949–1997). *J. Geophys. Res.,* **104,** 30 981–30 996.

Kurihara, Y., R. E. Tuleya, and M. A. Bender, 1998: The GFDL hurricane prediction system and its performance in the 1995 hurricane season. *Mon. Wea. Rev.,* **126,** 1306–1322.

Landsea, C. W., N. Nicholls, W. M. Gray, and L. A. Avila, 1996: Downward trends in the frequency of intense Atlantic hurricanes during the past five decades. *Geophys. Res. Lett.,* **23,** 1697–1700.

Manabe, S., R. J. Stouffer, M. J. Spelman, and K. Bryan, 1991: Transient response of a coupled ocean–atmosphere model to gradual changes of atmospheric CO_2. Part I: Annual mean response. *J. Climate,* **4,** 785–818.

Schade, L. R., and K. A. Emanuel, 1999: The ocean's effect on the intensity of tropical cyclones: Results from a simple coupled atmosphere–ocean model. *J. Atmos. Sci.,* **56,** 642–651.

Schimel, D., and Coauthors, 1996: Radiative forcing of climate change. *Climate Change 1995: The Science of Climate Change,* J. T. Houghton et al., Eds., Cambridge University Press, 65–131.

Shen, W., R. E. Tuleya, and I. Ginis, 2000: A sensitivity study of the thermodynamic environment on GFDL model hurricane intensity: implications for global warming. *J. Climate,* **13,** 109–121.

Siegel, S., and N. J. Castellan, 1988: *Nonparametric Statistics for the Behavioral Sciences,* 2d ed. McGraw-Hill, 399 pp.

Walsh, K. J. E., and B. F. Ryan, 2000: Tropical cyclone intensity near Australia as a result of climate change. *J. Climate,* **13,** 3029–3036.

Wentz, F. J., C. Gentemann, D. Smith, and D. Chelton, 2000: Satellite measurements of sea surface temperature through clouds. *Science,* **288,** 847–850.